Dynamics of fluxons in a system of two coupled Josephson transmission lines with local defects

1994 J. Phys.: Condens. Matter 6 9745

(http://iopscience.iop.org/0953-8984/6/45/023)

J. Phys.: Condens. Matter 6 (1994) 9745–9753. Printed in the UK

Dynamics of fluxons in a system of two coupled Josephson transmission lines with local defects

R Fokoua Tiwang, P Woafo and T C Kofané

Laboratoire de Mécanique, Faculté des Sciences, Université de Yaounde I, BP 812, Yaounde, Cameroon

Received 20 January 1994, in final form 18 May 1994

Abstract. We consider the dynamics of fluxons in two weakly coupled long Josephson transmission lines with localized impurities. The transmission, the pinning and the destruction of the bifluxon mode are obtained. In the case when there is a collision of a free fluxon belonging to one line with a pinned fluxon of the other line, we also observed three outcomes: capture of both fluxons; elastic collision; transmission of both fluxons at the impurity site.

1. Introduction

The study of fluxon propagation is a subject of considerable interest from both the theoretical and the practical point of view [1]. The unavoidable presence of various types of inhomogeneity which occur during the fabrication of Josephson transmission lines (JTLs) modifies the dynamical and structural properties of the fluxons. In the framework of perturbation theories for non-linear fields and the adiabatic approximation [2–4], the interaction may lead to the pinning of fluxons, the reflection and transmission of fluxons with distortion of the shape and a drastic change in the fluxon dynamical behaviour [5, 6].

In recent years, particular attention has been devoted to the propagation of fluxons in weakly coupled and perturbed JTLs [7–9]. It has been demonstrated that two colliding fluxons belonging to different lines can form a bound state owing to dissipative losses [7]. This is the bifluxon mode whose stability and dynamical behaviour during the interaction with local impurities is considered hereafter. The stability of the coupled model has also been investigated [9] and observation of phase-locking phenomena in self-resonant modes has been reported [8].

Our aim in this paper is twofold. Firstly, we study the stability and dynamics of the bifluxon mode in the presence of local impurities in both lines. Three possible outcomes are obtained: crossing of the bifluxon mode; capture of the bifluxon mode which leads to the generation of a new but stationary bifluxon mode with a reduced width; finally the destruction of the bifluxon mode due to pinning of one of the components of the bifluxon mode. Secondly, we consider the collision of a free fluxon in one line with a fluxon pinned by a microshort (or microresistor) in the other line. Three outcomes are also possible: capture of both fluxons; elastic collision; depinning of the pinned fluxon without the capture of the free fluxon. This last outcome leads to the formation of a bifluxon subsequently. The organization of the paper is as follows.

In section 2, we present the model and describe the bifluxon mode. Section 3 deals with the analysis of the bifluxon stability and dynamics during the interaction with the impurity. The collision of a fluxon belonging to one line with the pinned fluxon of the other line is

0953-8984/94/459745+09$19.50

considered in section 4. In section 5 we conclude and point out some interesting problems which have not been investigated.

2. The model and the bifluxon mode

The dynamics of fluxons in a system of two inductively coupled JTLs in the presence of local inhomogeneities are governed by the following system of two coupled and perturbed sine–Gordon equations [7]:

$$\phi_{i,tt} - \phi_{i,xx} + \sin\phi_i = P_i \tag{2.1}$$

where ϕ_i $(i = 1, 2)$ are the wavefunctions, P_i are the perturbation forces of the form

$$P_i = -f_i - \lambda\phi_{i,t} + \alpha\phi_{j,xx} - 2\epsilon\delta(x)\sin\phi_i \tag{2.2}$$

and $j = 1$ if $i = 2$ or $j = 2$ if $i = 1$. δ is the Dirac function. The subscripts x and t denote the derivative with respect to the normalized space unit x and time unit t, respectively. Here x and t are measured in units of [4] $\{\hbar/2eI_c[1-(M/L)^2]\}^{1/2}$ and $(\hbar C_1/2eI_c)^{1/2}$, respectively. $f_i = -I_{bi}/I_c$ are the normalized bias currents on each line; $\lambda_i = G\alpha_i(\hbar/2eI_c)^{1/2}$ are the dissipation coefficients due to tunnelling of normal electrons across the insulating barrier of the junctions (see [4] for details). The last term corresponds to a local inhomogeneity of the maximum Josephson current density (a microshort or a microresistor for positive or negative ϵ, respectively). Throughout the paper, the terms f_i, λ_i, α and ϵ are assumed small. In this model the surface loss in the superconductors as well as a capacitive coupling between lines are ignored.

In the absence of perturbations (i.e. $P_i = 0$), the system of equations (2.1) becomes two independent and exactly integrable sine–Gordon equations. The solutions corresponding to fluxons (or antifluxons) are

$$\phi_i(x, t) = 4\tan^{-1}\{\exp[\sigma_i(x - X_i)]\} \tag{2.3}$$

where $\sigma_i = \pm 1$ are the polarities of the fluxons and $X = X_{0i} + v_i t$ are the coordinates of the centres of the fluxons, X_{0i} being the initial positions of the centres and v_i the velocities of the fluxons.

In the weakly coupled model, it is known that the coupling between the lines leads to a small distortion in the shape of the fluxons, the well known image of a fluxon of one line in the other line [7, 10]. For the fluxon coordinates X_i, the McLaughlin–Scott [4] perturbation analysis leads to

$$\frac{d^2X_i}{dt^2} = \frac{\pi}{4}\sigma_i f_i - \lambda_i\frac{dX_i}{dt} - \frac{\alpha\sigma_i\sigma_j}{\sinh X_{ij}}\left(1 - \frac{X_{ij}}{\tanh X_{ij}}\right) \tag{2.4}$$

where $X_{ij} = X_i - X_j$ is the distance between the centres of the fluxons. Equations (2.4) have been studied in [7], where it is demonstrated that, owing to energy dissipative loss, and under some threshold conditions, the two fluxons can fuse into a bound state called a bifluxon with a constant velocity

$$v_b = \frac{\pi}{4}\frac{\sigma_1 f_1 + \sigma_2 f_2}{\lambda_1 + \lambda_2}. \tag{2.5}$$

The distance between the two fluxons (or antifluxons) bound into a bifluxon is

$$X_0 = \frac{3\pi}{8|\alpha|}(\sigma_1 f_1 - \sigma_2 f_2) \tag{2.6}$$

in the attractive case (i.e. $\alpha\sigma_1\sigma_2 > 0$) and

$$X_0 = \ln\left|\frac{16\alpha}{\pi(\sigma_1 f_1 - \sigma_2 f_2)}\right| \tag{2.7}$$

in the repulsive case (i.e. $\alpha\sigma_1\sigma_2 < 0$). For X_0 we have obtained expressions slightly different from that obtained by Kivshar and Malomed [7]. In the attractive case, our expression is 0.5 times their equation and, in the repulsive case, the argument of the Napierian logarithmic function should be multiplied by $\pi/16$ to obtain their function. These expressions ((2.6) and (2.7)) are in good agreement with the numerical simulation of equations (2.4).

3. Interaction of the bifluxon with impurities

To take into account the presence of the inhomogeneities on the coupled lines, we consider equations (2.1) with the full expressions of the perturbations P_i given in (2.2). We obtain, for the centres X_i of the fluxons, the following equations:

$$\frac{\mathrm{d}^2 X_i}{\mathrm{d}t^2} = \frac{\pi}{4}\sigma_i f_i - \lambda_i \frac{\mathrm{d}X_i}{\mathrm{d}t} - \frac{\alpha\sigma_i\sigma_j}{\sinh X_{ij}}\left(1 - \frac{X_{ij}}{\tanh X_{ij}}\right) + \epsilon\sigma_i \operatorname{sech}^2 X_i \tanh X_i. \tag{3.1}$$

In the absence of the coupled junction (i.e. $\alpha = 0$), the velocity of the uniform motion (i.e. $\epsilon = 0$) is given by

$$v_{i\infty} = \frac{\pi\sigma_i f_i}{4\lambda}. \tag{3.2}$$

The impurity in this case can pin the fluxon provided that the condition

$$f_i < f_{ic} = \frac{4\lambda_i}{\pi}\sqrt{\epsilon} \tag{3.3}$$

obtained by energy considerations is satisfied [4].

In the case of coupled junctions, we have seen that a bifluxon can be formed, and it is stable until it reaches the close vicinity of the defect. No matter how small the defect is, it breaks the bifluxon. This makes analytical predictions rather complicated for the bifluxon mode. However, the study is done numerically using the fourth-order Runge–Kutta method. This provides three possible outcomes at the impurity site: crossing of both fluxons (components of the previous bifluxon); pinning of one fluxon; pinning of both fluxons (figure 1). This is due to the influence of three potentials acting upon the fluxons at the vicinity of the impurity: the coupling potential between the fluxons given by

$$U = 8\alpha\sigma_i\sigma_j \frac{X_{ij}}{\sinh X_{ij}} \tag{3.4}$$

the impurity potential given by

$$U_i = 4\epsilon\sigma_i \operatorname{sech}^2 X_i \tag{3.5}$$

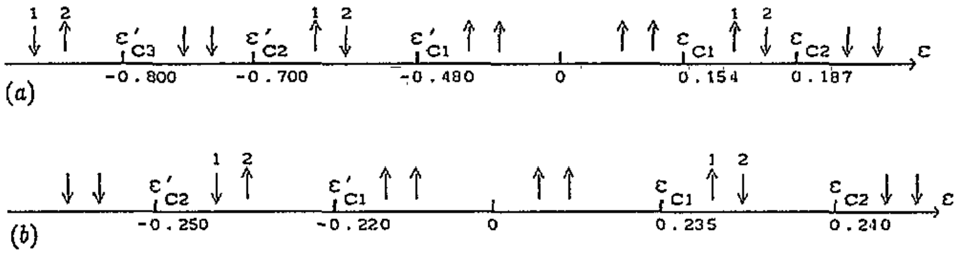

Figure 1. Outcomes of the collision for (*a*) the fluxon–fluxon bound state and (*b*) the fluxon–antifluxon bound state. The downward arrow means a pinned wave, and the upward arrow a transmitted wave. Wherever there could be confusion, the numbers on top of each arrow indicate which of the waves is transmitted or pinned. The parameters are as follows: $\alpha = 0.1$, $\lambda_1 = \lambda_2 = 0.1$, $f_1 = 0.04$, (*a*) $f_2 = 0.05$ and (*b*) $f_2 = -0.05$.

and obviously the potential due to the driving forces f_i.

We have assumed that the bifluxon approaches the impurity from large negative values of X_i (the impurity being localized at the site $X_i = 0$ as can be seen from the Dirac delta function in equation (2.2)) and moving with constant velocity v_b given by equation (2.5). The outcomes are the same for attractive and repulsive coupling between the fluxons, and attractive and repulsive inhomogeneities, but with different critical values of the height ϵ of the impurity barrier. We give here a discussion of the results obtained during the numerical computation. In what follows, we shall for purposes of fluency and clarity refer to fluxons by their centres X_1 and X_2. The case of the fluxon–fluxon bound state and the fluxon–antifluxon bound state are qualitatively different. In fact, in the former case, the impurity is either repulsive or attractive to both fluxons while, in the latter case, the impurity is attractive to one fluxon and repulsive to the other fluxon.

3.1. *Case of a fluxon–fluxon bound state* ($\sigma_1 = \sigma_2 = 1$)

The interaction of the bifluxon with the attractive ($\epsilon < 0$) and the repulsive ($\epsilon > 0$) impurities is summarized in figure 1(*a*) for a fluxon–fluxon bound state. The study is carried out for a set of fixed parameters (see figure 1), which describes the general phenomena observed for such interactions. We mainly study the influence of the intensity of the amplitude ϵ of the impurity potential on the motion of the coupled fluxons. The study provides some critical values of this amplitude, which subdivide the axis of ϵ into firstly regions of crossing of both fluxons where they reconstitute the broken bifluxon long after they have passed the defect, secondly regions where only one of the fluxons is allowed to pass the impurity barrier, the other undergoing a damped oscillatory motion before or after the impurity site, depending on whether the impurity is repulsive or attractive to it, and to settle (i.e. $v_f = 0$) finally close to the impurity site, and thirdly regions where the two fluxons are pinned, forming a different and stationary bifluxon ($v_b = 0$) near the impurity site. These values are represented in figure 1 by ϵ_{c1} (or ϵ'_{c1} for negative ϵ) below (or above) which the waves get over the impurity barrier; the second and third regions are separated by ϵ_{c2} (or ϵ'_{c2} for negative ϵ) above (or below) which the two waves are pinned. For this last outcome, we have plotted the time variation in the width $X_{ij}(t)$ of the bifluxon in figure 2 for $\epsilon = 0.19$, where one can see that the final value of X_{ij} is negative, implying that X_2 is pinned at a closer distance to the defects than X_1 is, simply because, with the set of parameters used, the driving force f_2 is greater than f_1 and thus can better resist the repulsive impurity. The case of negative ϵ provides a third critical value ϵ'_{c3} below which the inverse of the phenomenon of the second region is observed; that is X_2 which was pinned in the second region (i.e. $\epsilon'_{c2} < \epsilon < \epsilon'_{c1}$) now passes while X_1 is pinned (see figure 1(*a*)). A reasonable explanation for this situation is that, when the waves are drawn back by the attractive impurity, X_2 happens to pass ahead of X_1 during their oscillations and the driving force f_2, which is stronger than f_1, combined with the attractive coupling potential cause X_2 to go through the impurity.

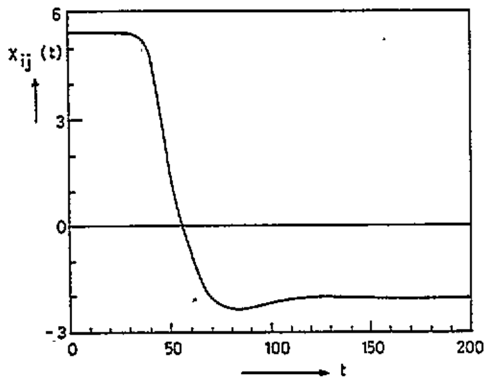

Figure 2. Variation versus time of the bifluxon width $X_{ij}(t)$ in the case of a pinned bifluxon for $\epsilon = 0.19$ and the parameters in figure 1(*a*).

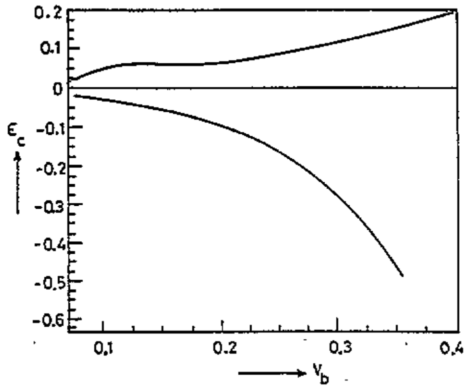

Figure 3. Critical value ϵ_c versus the bifluxon velocity for $\alpha = \lambda_1 = \lambda_2 = 0.1$.

We have plotted in figure 3 the graph of ϵ_c (the critical values of ϵ below which the bifluxon mode is transmitted through the inhomogeneity) versus the velocity v_b of the bifluxon for both the attractive and the repulsive inhomogeneity to the bound state of fluxons. It is observed in figures 1 and 3 that the critical values of ϵ for attractive defects are greater than for the repulsive defects. This clearly shows that it is easier for the fluxons to pass an attractive defect than a repulsive defect.

3.2. *Case of a fluxon–antifluxon bound state*

Another interesting case that has attracted our attention is where the two waves have opposite polarities. In our study the fluxon is represented by X_1 ($\sigma_1 = 1$) and the antifluxon by X_2 ($\sigma_2 = -1$). For $\alpha = 0$, equation (3.2) gives the velocity $v_{i\infty}$ of the uniform motion of the non-relativistic fluxons. This expression for $v_{i\infty}$ shows that the antifluxon X_2 will be driven to the right by a negative force f_2. The coupling potential between the two waves becomes attractive for $\alpha > 0$. Figure 1(*b*) gives the outcomes of the interactions of this bifluxon with the attractive and with the repulsive inhomogeneity. They are qualitatively the same as for the fluxon–fluxon bound state; however, the various regions do not have the same lengths in both cases.

The case of a negative coupling coefficient ($\alpha < 0$) although not suitable for the JTL ($\alpha = M/L$ being positive), but interesting in the coupled monatomic chains of particles, e.g. the Frenkel–Kontorova model or adatomic chains [10–12], has led to outcomes similar to those presented above.

4. Interaction between a free and a pinned fluxon near the local inhomogeneity

In this section we study the interaction between a free fluxon and a pinned fluxon. It is assumed that the first line bearing X_1 has no impurity; the second line contains an impurity localized at the site $X_2 = 0$ near which X_2 is initially pinned. The stationary coordinate X_{20} of the pinned fluxon is determined by solving the equation

$$\frac{\mathrm{d}U_{\mathrm{eff}}}{\mathrm{d}X_2} = 0 \tag{4.1}$$

where

$$U_{\mathrm{eff}} = -2\pi\sigma_2 f_2 X_2 + 4\epsilon\sigma_2 \operatorname{sech}^2 X_2 \tag{4.2}$$

since X_1 is initially far from X_2. Solutions to equation (4.1) exist if the condition (3.3) is satisfied.

One of the main purposes of this section is to find critical conditions for the depinning of the pinned fluxon. A similar study has been made by Malomed and Nepomnyashchy [13]. Their study was undertaken in the case where the two waves belong to the same line and thus interact through another type of potential. They demonstrated that, in the case of like polarities of the fluxons, three different outcomes of the collision were possible: capture of both fluxons; capture of the free fluxon and depinning of the pinned fluxon, which they called exchange; finally depinning of the pinned fluxon without capture of the free fluxon. In the case of opposite polarities, the outcomes of the collisions were depinning, elastic collision, and annihilation of the fluxon–antifluxon pair.

In our coupled model, the equations of motion are as follows:

$$\frac{\mathrm{d}^2X_1}{\mathrm{d}t^2} = \frac{\pi}{4}\sigma_1 f_1 - \lambda_1\frac{\mathrm{d}X_1}{\mathrm{d}t} - \frac{\alpha\sigma_1\sigma_2}{\sinh X_{12}}\left(1 - \frac{X_{12}}{\tanh X_{12}}\right) \tag{4.3a}$$

$$\frac{\mathrm{d}^2X_2}{\mathrm{d}t^2} = \frac{\pi}{4}\sigma_2 f_2 - \lambda_2\frac{\mathrm{d}X_2}{\mathrm{d}t} + \frac{\alpha\sigma_1\sigma_2}{\sinh X_{12}}\left(1 - \frac{X_{12}}{\tanh X_{12}}\right) + \epsilon\sigma_2 \operatorname{sech}^2 X_2 \tanh X_2. \tag{4.3b}$$

The stationary solutions of (4.3), which may be seen as the state at which the two fluxons are pinned near the impurity, are obtained by setting $\mathrm{d}^2X_i/\mathrm{d}t^2 = \mathrm{d}X_i/\mathrm{d}t = 0$. The numerical study shows that, for certain values of the impurity amplitude ϵ (for which condition (3.3) is not fulfilled), the set of equations (4.3) has no stationary solution, implying that the two fluxons cannot be held by the impurity. The initial conditions to compute the dynamical solutions of equations (4.3) are the following: at $t = 0$, X_1 is far from the impurity site with an initial velocity $v_i = \pi\sigma_1 f_1/4\lambda$ and $X_2 = X_{20}$, $v_2 = 0$, where X_{20} is the pinning point of X_2 (i.e. the stable solution of equation (4.2)).

The study provides three outcomes at the impurity site: capture, i.e. pinning of the free fluxon with the pinned fluxon remaining pinned; depinning of the initially pinned fluxon without capture of the free fluxon; elastic collision, i.e. the free fluxon passes the defect and the pinned fluxon remains pinned.

4.1. Interaction between fluxons with like polarities

We discuss here the general result for both the barrier ($\epsilon > 0$) and the well ($\epsilon < 0$) of the potential since the outcomes are qualitatively the same for both cases. It is obvious

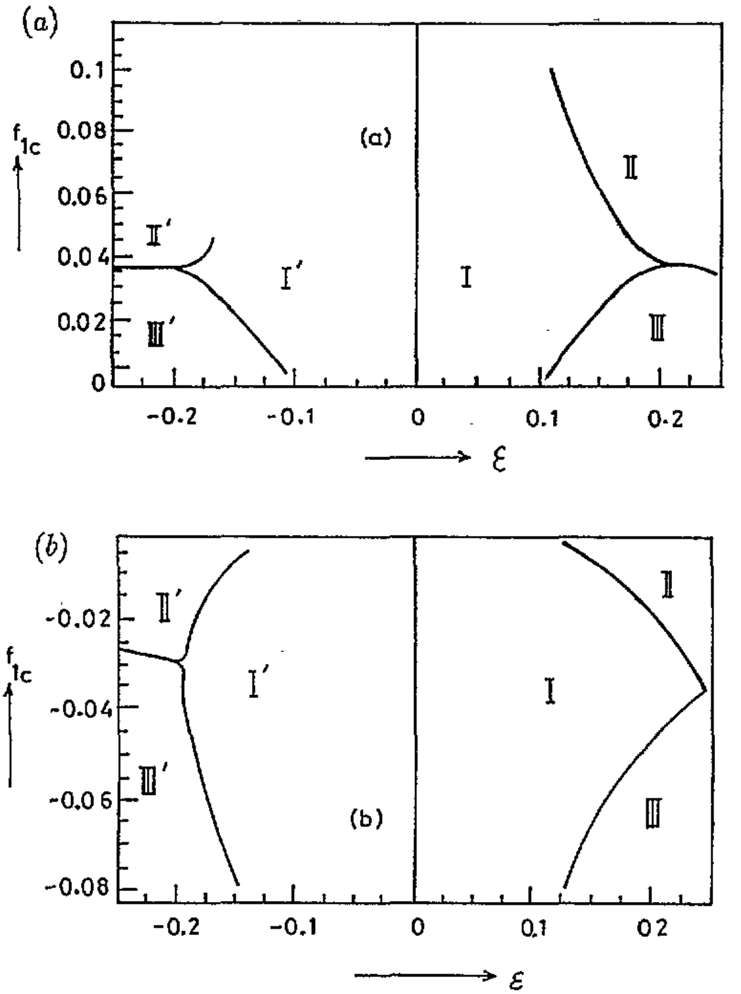

Figure 4. Interaction regimes in the case of (*a*) the incoming fluxon and (*b*) the incoming antifluxon for the repulsive and the attractive impurity with $f_2 = 0.05$; regions I and I′, transmission of both fluxons; regions II and II′, elastic collision; regions III and III′, pinning of both fluxons.

that, if the kinetic energy of the free fluxon is not sufficient compared with the repulsive coupling with the pinned X_2, X_1 will be pinned. This means that there is a critical value of f_1 (f_{1d} since the velocity of the fluxon's uniform motion depends on f_1) beneath which X_1 cannot pass the impurity region (it will necessarily be pinned because the driving and coupling forces acting upon it have opposite directions). This critical value f_{1d} increases with increasing height (or depth) ϵ of the impurity potential. Beyond and above f_{1d}, X_1 depins X_2. Depinning is observed until another critical value f_{1e} is reached where the depinning ceases and elastic collision takes over. Unlike f_{1d}, f_{1e} decreases with increasing $|\epsilon|$. In figure 4 we have plotted the graph of f_{1c} versus ϵ; the variations in f_{1d} are represented by the lower branches of the curves while the upper branches represent the variations in f_{1e}. The depinning zone $F_1 = |f_{1d} - f_{1e}|$ decreases as ϵ increases, and finally vanishes for $\epsilon = \epsilon_c$ ($\epsilon_c = 0.18$ in figure 4(*a*) for example). Figure 5 shows the graph of the pinning potential U_{eff} for $\epsilon = -0.13$ and for $\epsilon = -0.10$. For small values of ϵ the potential has no equilibrium position. For greater values of ϵ there are two extrema corresponding to the stable and unstable pinning positions of X_2. As X_1 goes into the impurity area, it shifts X_2. If X_2 exceeds the unstable equilibrium position, depinning is observed; if not, we have either capture or elastic collision.

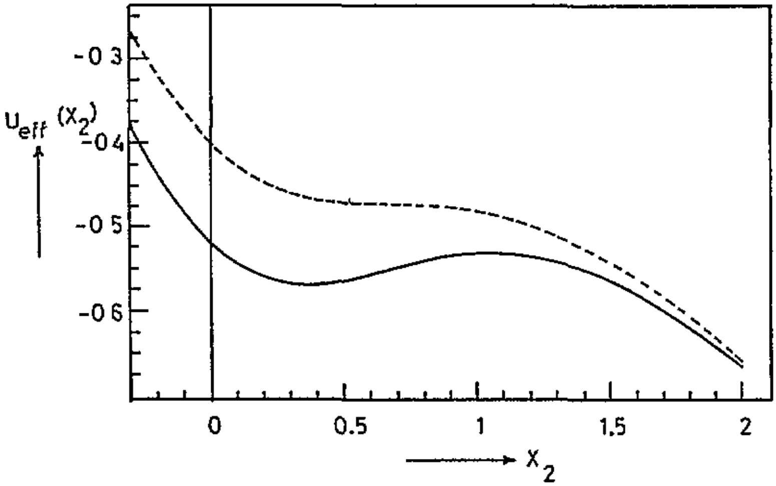

Figure 5. The effective pinning potential U_{eff} for X_2 with $f_2 = 0.05$ for $\epsilon = -0.10$ (- - - -) and $\epsilon = -0.13$ (——).

4.2. *Interaction between fluxons with opposite polarities*

In the general case, this collision provides the same outcomes as in section 4.1. It is observed that the depinning zone $F_1 = |f_{1d} - f_{1e}|$ is larger than in the case of like polarities (see figure 4). This is due to the attraction between the two waves that makes the depinning easier than in the case of like polarities.

5. Conclusion

In this paper, we have studied the interaction of fluxons belonging to two inductively coupled JTLs with localized impurities. Using the McLaughlin–Scott [4] perturbation theory, we have simulated numerically the coupled differential equations of the fluxon coordinates perturbed by the impurity forces. Three outcomes have been obtained: transmission, pinning, and destruction of the bifluxon mode. In the case of the collision of a free fluxon belonging to one line with a pinned fluxon of the other line, we have also obtained three possible outcomes: capture of both fluxons, elastic collision, and transmission of both fluxons at the impurity site.

Our study is effected in a non-relativistic limit. Also, we have not considered the newly established resonant interactions between fluxons and the generated impurity mode as well as radiative losses [5, 14]. However, in real systems such as ours, the dissipative losses and the bias currents will destroy the resonant structure since the impurity mode will fade after their excitation [14]. On the other hand, direct numerical simulation of the inhomogeneous coupled equations (2.1) with additional coupling (e.g. the capacitive coupling and the surface losses), as well as an experiment on the coupled inhomogeneous JTL, should be carried out to determine the accuracy of our results. It would also be interesting to undertake a study in the relativistic limit where it has recently been shown in a one-dimensional sine–Gordon model [15] that the soliton width can be altered through interactions with a localized substrate potential. Moreover, direct numerical simulation of (2.1) will help us to compute the currents and voltages of the junctions around the localized impurity.

References

[1] Barone A and Paterno G 1982 *Physics and Applications of the Josephson Effect* (New York: Wiley)
[2] Fogel M B, Trullinger S E, Bishop A R and Krumhansl J A 1977 *Phys. Rev.* B **15** 1578
[3] Kaup D J and Newell A C 1978 *Proc. R. Soc.* A **361** 413
[4] McLaughlin D W and Scott A C 1978 *Phys. Rev.* A **18** 1652
[5] Kivshar Y S and Malomed B A 1989 *Rev. Mod. Phys.* **61** 763
[6] Woafo P and Kofané T C 1993 *Phys. Scr.* **47** 280
[7] Kivshar Y S and Malomed B A 1988 *Phys. Rev.* B **37** 9324
[8] Holst T, Hancen J B, Grønbech-Jensen N and Blackburn J A 1990 *Phys. Rev.* B **42** 127
[9] Grønbech-Jensen N, Samuelsen M R, Lomdahl P S and Blackburn J A 1990 *Phys. Rev.* B **42** 3976
[10] Woafo P, Kofané T C and Bokosah A S 1992 *J. Phys.: Condens. Matter* **4** 809
[11] Braun O M, Kivshar Y S and Kosevich A M 1988 *J. Phys. C: Solid State Phys.* **21** 3881
[12] Woafo P and Kofané T C 1993 *J. Phys.: Condens. Matter* **5** 4137
[13] Malomed B A and Nepomnyashchy A A 1992 *Phys. Rev.* B **45** 1243
[14] Zhang Fei, Kivshar Y S, Malomed B A and Vasquez L 1991 *Phys. Rev. Lett.* A **159** 318
Zhang Fei, Kivshar Y S and Vasquez L 1992 *Phys. Rev.* A **45** 6019; 1992 *Phys. Rev.* A **46** 5214
Zhang L, Huang L and Qiu M X 1993 *Phys. Rev.* B **47** 1088
[15] Woafo P and Kofané T C 1994 *Solid State Commun.* **89** 261